Global event-triggered regulation of unicycle dynamics by bounded control

Denis Efimov, Mata Khalili, Shiyu Liu

Global event-triggered regulation of unicycle dynamics by bounded control

Denis Efimov, Mata Khalili, Shiyu Liu

***Abstract*—The problem of stabilization of the position of a mobile robot using its cinematic (unicycle type) model is considered. The suggested control is discontinuous and bounded; moreover, it guarantees a global solution to the posed problem. The properties of the proposed control law are analyzed by applying the Lyapunov function method. An event-triggering realization of the control algorithm is presented, and its performance and tuning are evaluated through simulations.**

***Index terms*—** Event-triggered control, networked control systems, mobile robots

I. Introduction

The navigation problem for mobile robots has plenty of solutions [1]. The diversity of control laws proposed in the literature can be attributed to the presence of different constraints and performance criteria within the field of robotics [2]. Additionally, conventional and widely adopted cinematic models for wheeled mobile robots, known as the unicycle model, is characterized by the lack of controllability, a facet that is studied in this work. For this class of dynamics, regulation of the complete state vector to a desired position via a continuous state feedback is impossible [3], then different time-varying or discontinuous solutions exist in the literature [4], [5], [6], [7], [8]. One common approach to address this structural challenge is to shift focus from stabilization to tracking control [9], [10], which inherently introduces time-varying control. Another approach proposes to relax the regulation goal asking merely for control of the position, but not the orientation of the robot at the final destination, then continuous feedback may become possible [11]. Important characteristics in applications are the boundedness of the control, since robot motors cannot generate an arbitrary amplitude torques, which becomes a challenging issue if a global (or under sufficiently big deviations) regulation of robots is considered [12], [13], [14]. Note that most existing control laws are either not bounded or not global, or their applicability is based on rather sophisticated hypotheses.

In the case of distant navigation of a mobile robot, when a centralized planner is applied that makes a unified supervision of the fleet of different mobile agents, then an additional important constraint appears, which deals with the network load by control and estimation algorithms. Extensive usage of the communication channel by different distributed navigation/monitoring tools and agents may lead to channel saturation and packet losses, which results in the degradation of the quality of service and the appearance of significant delays [15]. One strategy to alleviate network load is through sampled or event-triggered (ET) control and estimation [16], [17], [18], [19], updating information only when certain conditions are violated. This guarantees the system's proper and desirable performance. A popular and simple method for embedding the existent feedback solutions to ET setup is based on the utilization of a Lyapunov function, which ensures the stability of the control in the continuous-time case [20], [21].

In this work, we consider the problem of positioning global regulation to a point for a unicycle (without final constraint on its orientation) applying bounded control, with its posterior immersion to the ET framework. Roughly speaking, we assume that a global planner provides us with a set of waypoints, and the robot has to follow them in the desired order without any special restrictions on the behavior in between. This approach facilitates the integration of this control strategy with a collision avoidance algorithm. In the case of trajectory tracking, it may be necessary to replan the desired trajectory after a collision avoidance event. However, as long as the next set of waypoints is available, no replanning or intervention from the global planner is required, thereby conserving computational and communication resources. Boundedness of the control allows the robot to navigate globally while staying close to the maximal admissible velocity (if the control is saturated in almost all operation domains), whereas ET serves for minimization of the communication load, as has been explained above. To this end, first, we propose a discontinuous bounded global stabilizer of the position with a strict Lyapunov function (the discontinuity region is not transgressed during the transients, thus, the control signal stays continuous on each particular trajectory). Secondly, using the approach from [20], an ET scheme is formulated. Finally, the control tuning and the performance of ET regulation are investigated through numeric simulations under Matlab/Simulink environment.

The outline of this paper is as follows. The problem statement is given in Section II. The design of a bounded global stabilizer of the unicycle's position is presented in

Denis Efimov is with Inria, Univ. Lille, CNRS, UMR 9189 - CRIStAL, F-59000 Lille, France.

Mata Khalili and Shiyu Liu are with Nokia Bell Labs Paris Saclay, 91300 Massy, France.

Section III, where the analysis is based on utilization of a Lyapunov function method. An ET implementation of the proposed bounded feedback is investigated in Section IV. The tuning of control parameters and their influence on the transients are evaluated by computer experiments, and discussed in Section V. We finally demonstrate in Section VI the control performance with an ET scheme.

Notation

Denote by $\mathbb{R}$ and $\mathbb{Z}$ the set of real and integer numbers respectively, $\mathbb{Z}_+ = \{j \in \mathbb{Z} : j \geq 0\}$.

The symbol $|\cdot|$ is used to denote the absolute value of a real.

The definitions of the used stability properties and notions can be found in [22].

II. Problem statement

Consider a mobile robot, whose dynamics can be presented by the unicycle cinematic model:

$$\begin{aligned} \dot{x}(t) &= u_1(t)\cos(\theta(t)), \\ \dot{y}(t) &= u_1(t)\sin(\theta(t)), \\ \dot{\theta}(t) &= u_2(t), \end{aligned} \tag{1}$$

where $x(t), y(t) \in \mathbb{R}$ determine the robot's position on the plane, and $\theta(t) \in [-\pi, \pi)$ is the heading angle that tabulates the orientation, $X(t) = [x(t), y(t), \theta(t)]^\top$ denotes the state vector of the system; $u_1(t) \in [-u^1_{\max}, u^1_{\max}], u_2(t) \in [-u^2_{\max}, u^2_{\max}]$ are bounded controls corresponding to linear and angular velocities, respectively, with $u^1_{\max} > 0$ and $u^2_{\max} > 0$ being the maximal admissible control amplitudes, $U(t) = [u_1(t), u_2(t)]^\top$; $t \geq 0$.

Problem. Design a bounded ET state feedback $u_1(t) = u_1(X(t))$ and $u_2(t) = u_2(X(t))$ globally stabilizing any given neighborhood of the set $\mathcal{O} = \{X \in \mathbb{R}^2 \times [-\pi, \pi) : x = y = 0\}$ for (1).

This problem will be solved in two steps: first, a global bounded discontinuous feedback stabilizing $\mathcal{O}$ for (1) will be synthesized (the angle θ is not constrained when the position $x = y = 0$ is reached); second, an ET mechanism will be proposed using the Lyapunov function methodology [20]. Note that the practical regulation of the set $\mathcal{O}$ is demanded in order to avoid an infinite commutation at this set, if Zeno behavior is admissible, then the same ET control can guarantee the exact asymptotic convergence to $\mathcal{O}$.

III. Global bounded stabilizer at the origin

In this section we propose a bounded state feedback $U(X)$ providing asymptotic stability of the closed-loop system at $\mathcal{O}$.

Let us define the desired orientation of the robot as

$$\theta_d(t) = \arctan\left(\frac{y(t)}{x(t)}\right) - \pi,$$

then the heading $\theta(t) = \theta_d(t)$ implies that the robot looks exactly to the point $x = y = 0$ (further, in this section the time dependence of the variables will be omitted for brevity). Recalling the formulas $\cos(\arctan(\phi)) = \frac{1}{\sqrt{1+\phi^2}}$ and $\sin(\arctan(\phi)) = \frac{\phi}{\sqrt{1+\phi^2}}$ that are satisfied for any $\phi \in \mathbb{R}$, the following useful equalities can be established:

$$\begin{aligned} x\cos(\theta_d) + y\sin(\theta_d) &= -\sqrt{x^2+y^2}, \\ x\sin(\theta_d) - y\cos(\theta_d) &= 0. \end{aligned} \tag{2}$$

To design the control laws we use a simple quadratic Lyapunov function:

$$V(X) = x^2 + y^2 + \gamma(\theta - \theta_d)^2,$$

where $\gamma > 0$ is a parameter whose role will be clarified in the next section. The function V is continuous and positive definite for $\theta - \theta_d \in [-\pi, \pi)$ (*i.e.*, $V(X) = 0$ implies $X \in \mathcal{O}$), but it is not continuously differentiable for $|\theta - \theta_d| \to \pi$. Calculating the derivative of V along the trajectories of (1) we obtain:

$$\begin{aligned} \dot{V} &= 2x\dot{x} + 2y\dot{y} + 2\gamma(\theta - \theta_d)(\dot{\theta} - \dot{\theta}_d) \\ &= 2u_1(x\cos(\theta) + y\sin(\theta)) + 2\gamma(\theta - \theta_d)(u_2 - \dot{\theta}_d) \\ &\coloneqq W(X, U), \end{aligned} \tag{3}$$

where straightforward computations show that

$$\dot{\theta}_d = u_1 \frac{x\sin(\theta) - y\cos(\theta)}{x^2 + y^2}. \tag{4}$$

Let us select the control laws in the form:

$$u_1(X) = -\rho(\theta - \theta_d)\varphi_1\left(k_1(x\cos(\theta) + y\sin(\theta))\right), \tag{5}$$

$$u_2(X) = -\varphi_2\left(k_2(\theta - \theta_d) - \frac{\dot{\theta}_d}{u^2_{\max}}\right),$$

where

$$\varphi_i(s) = u^i_{\max}\begin{cases} s & \text{if } |s| \leq 1 \\ \operatorname{sign}(s) & \text{if } |s| > 1 \end{cases}, \ i = 1, 2,$$

$$\rho(s) = \exp(-\eta s^2),$$

and $k_1 > 0$, $k_2 > 0$, and $\eta > 0$ are tuning gains, whose values will be constrained later. Note that the control u_2 may be discontinuous while $|\theta - \theta_d| \to \pi$.

Remark 1. The intuition behind the appearance of ρ is to decrease the linear velocity of the robot u_1 for big deviations of θ from its desired value θ_d (and when the control u_1 in (5) takes negative values), which can be regulated by adjusting the value of η. The gains k_1 and k_2 enlarge the domain where the maximal amplitude of the control $u^i_{\max}$, $i = 1, 2$ is applied by (5).

By construction, the following properties are satisfied for all $X \in \mathbb{R}^2 \times [-\pi, \pi)$:

$$\begin{aligned} 0 < \exp(-\eta\pi^2) \leq \rho(\theta - \theta_d) \leq 1, \\ -u^i_{\max} \leq \varphi_i(s) \leq u^i_{\max}, \ i = 1, 2, \ \forall s \in \mathbb{R}, \end{aligned}$$

hence,

$$-u^i_{\max} \le u_i(X) \le u^i_{\max},\ i=1,2.$$

Moreover, several less obvious relations can be observed:

Lemma 1. *For any $X \in \mathbb{R}^2 \times [-\pi,\pi)$,*

$$|\dot\theta_d| \le \kappa_{\max}|\theta-\theta_d|$$

with $\kappa_{\max} = \sqrt{2}k_1u^1_{\max}$.

All proofs are excluded due to space limitations.

Lemma 2. *There exists $\eta>0$ such that*

$$|\dot\theta_d| \le \kappa_{\min} < u^2_{\max} \tag{6}$$

for all $x\in\mathbb{R}$, $y\in\mathbb{R}$ and all $|\theta-\theta_d| \ge \frac{1}{k_2+(u^2_{\max})^{-1}\kappa_{\max}}$, where

$$\kappa_{\min} = \kappa_{\max}\max\left\{\frac{e^{-0.5}}{\sqrt{2\eta}}, \frac{e^{\frac{-\eta}{(k_2+(u^2_{\max})^{-1}\kappa_{\max})^2}}}{k_2+(u^2_{\max})^{-1}\kappa_{\max}}\right\}.$$

Note that the satisfaction of (6) can be guaranteed by tuning the value of η:

$$\eta > \max\left\{\exp(-1)\left(\frac{k_1u^1_{\max}}{u^2_{\max}}\right)^2, \right. \tag{7}$$
$$\left. -\left(k_2+\frac{\kappa_{\max}}{u^2_{\max}}\right)^2\ln\left(\frac{u^2_{\max}\left(k_2+\frac{\kappa_{\max}}{u^2_{\max}}\right)}{\kappa_{\max}}\right)\right\}.$$

Using lemmas 1 and 2, straightforward calculations show that for

$$k_2 > (u^2_{\max})^{-1}\kappa_{\max} = \sqrt{2}k_1\frac{u^1_{\max}}{u^2_{\max}} \tag{8}$$

the inequality $\dot V<0$ is satisfied for all $x^2+y^2\neq 0$ and $\theta\neq\theta_d$, which ensures boundedness of the state X and global asymptotic convergence of all trajectories in (1), (5) to the set $\mathcal{O}$. Note that the line $\theta=\theta_d$ is not transgressed by the trajectories of the closed-loop system, hence, there is no problem with discontinuity of the control u_2 (the solutions are well defined, and there is no chattering).

Therefore, the following result can be proven:

Theorem 1. *For any given $u^i_{\max}$, $i=1,2$ and $k_1>0$, let $k_2>0$ be chosen to verify* (8) *while $\eta>0$ to guarantee* (6)*, then all trajectories of* (1)*,* (5) *are bounded and the set $\mathcal{O}$ is the global asymptotic attractor in $X\in\mathbb{R}^2\times[-\pi,\pi)$.*

Remark 2. Note that the restrictions obtained for the values of $\kappa_{\max}$, $\kappa_{\min}$, k_2 and η are very conservative and they are mainly indicating the reasons why these quantities exist. For implementation, it is better to adjust them based on numerical experiments (using the error and trial method).

IV. Event-triggering regulation

Let us consider how the control (5) can be implemented using the event-triggered framework.

Assume that the control of the robot (1) is realized through sampling-and-hold mechanism, thus, there exists a sequence of time instants t_k, $k\in\mathbb{Z}_+$ such that $t_{k+1}>t_k\ge t_0=0$ and $u_i(t)=u_i(t_k)$ for all $t\in[t_k,t_{k+1})$. The regulation problem stays the same, that is stabilization of any given neighborhood of the set $\mathcal{O}$. We assume that the commutation instants t_k can be selected by the designed ET mechanism, and the objective of triggering consists in minimization of the number of switchings during the transients.

To this end, according to the conventional ET results [19], [20], let us select the following supervision algorithm for $\sqrt{x^2(t_k)+y^2(t_k)}>\varepsilon$:

$$t_{k+1} = \arg\inf_{t>t_k}\{\sqrt{x^2(t)+y^2(t)}\le\varepsilon \text{ or } W(X(t),U(t_k)) \ge \alpha W(X(t),U(t))\}, \tag{9}$$

where $\varepsilon>0$ and $\alpha\in(0,1]$ are tuning parameters, W is defined in (3) and $U(t)=[u_1(X(t)),u_2(X(t))]^\top$ by (5), $X(t)$ is the current measurement of the state, and

$$U(t_k) = \begin{cases} \begin{bmatrix}0\\0\end{bmatrix} & \text{if } \sqrt{x^2(t_k)+y^2(t_k)}\le\varepsilon \\ \begin{bmatrix}u_1(X(t_k))\\u_2(X(t_k))\end{bmatrix} & \text{otherwise}\end{cases}, \tag{10}$$

where again u_1 and u_2 are defined in (5), ε determines the neighborhood of the set $\mathcal{O}$ that is stabilized, then the control (the velocities of the robot) is set to zero once it is reached. During the transients, the derivative of the Lyapunov function V calculated in (3) for the frozen control $W(X(t),U(t_k))$ is compared with the one obtained for (1), (5), namely $W(X(t),U(t))$; if $W(X(t),U(t_k))<\alpha W(X(t),U(t))\le 0$ then the new event is not generated and the triggered control is not updated (according to the result of Theorem 1 we know that $W(X(t),U(t))$ is negative for any $x^2(t)+y^2(t)\neq 0$ and $\theta(t)\neq\theta_d(t)$, hence, $W(X(t),U(t_k))$ is guaranteed to stay negative). The parameter α characterizes the admissible deviation of the decay of $V(t)$ by $U(t_k)$ with respect to one provided by the nominal control law $U(t)$.

Since $\varepsilon>0$ and $\alpha>0$, and $-W(X(t),U(t))$ admits a lower bound as a function of the distance to the set $\mathcal{O}$, i.e., in terms of $\sqrt{x^2(t)+y^2(t)}$, then $t_{k+1}>t_k$ and the Zeno behavior is impossible.

Theorem 2. *Assume that all conditions of Theorem 1 are verified, then for any $\varepsilon>0$ and $\alpha>0$ all trajectories in* (1) *with the triggered control* (9)*,* (10) *stay bounded and there is a finite index $k^*=k^*(X(0))\ge 0$ such that $\sqrt{x^2(t_{k^*})+y^2(t_{k^*})}\le\varepsilon$.*

The role of the parameter γ introduced in V consists in weighting the angle regulation part $(\theta-\theta_d)^2$ over the positioning component of V to generate the control scheduling in

(9) providing reasonable deviations of the trajectories from the nominal ones. The former term is globally bounded by $2\gamma\pi(u^2_{\max} + \kappa_{\max}\pi)$ for $\theta - \theta_d \in [-\pi, \pi)$, while the latter can be unbounded for $x, y \in \mathbb{R}$.

V. Role of control parameters

Let us evaluate the role and significance of the control parameters in simulations while illustrating the control algorithm's performance

We have established a set of evaluation metrics to assess the impact of control parameter tuning under the diverse conditions mentioned afterwards, as described below.

1) **Speed indicator**: This metric assesses the speed at which the robot can navigate between the waypoints and reach its intended goal.
   It is calculated using the formula
   $$m_s = \frac{s}{T\, u^1_{\max}},$$
   where s is the total traveled distance, T is the total traveling time, and $u^1_{\max}$ is the maximum admissible linear velocity.
2) **Distance indicator**: This indicator assesses the extent of deviation of the robot from the straight line connecting the two waypoints, which evaluates the necessary space range for the robot's movement while capturing the smoothness of the traversed trajectory. The formula used is:
   $$m_d = \frac{s}{d},$$
   where s is the total traveled distance, and d is the shortest distance between two waypoints.
3) **Heading indicator**: This metric is formulated to compute the accumulated heading corrections normalized by the expected heading correction at the initial state. It aims to evaluate the speed at which the robot aligns its heading towards the goal and the smoothness of the heading variation throughout its trajectory.
   $$m_h = \frac{1}{|\theta_{init} - \theta^{\mathrm{d}}_{init}|} \int_0^T |\theta(t) - \theta^{\mathrm{d}}(t)| dt,$$
   where $|\theta_{init} - \theta^{\mathrm{d}}_{init}| := \tilde{\theta}_{init}$ is the degree of variance between the initial and desired heading when the robot is directed towards the goal, $|\theta(t) - \theta^{\mathrm{d}}(t)|$ indicates the instantaneous deviation in heading from the intended direction toward the goal. It should be noted that the operation $|\theta|$ represents the norm of an angle θ whose range is wrapped within $(-\pi, \pi]$.

Our objective in choosing control parameters is to maximize the speed indicator, while minimizing the distance and heading indicators. We conducted a series of simulations in Matlab/Simulink environment, by varying the three control parameters (*i.e.*, k_1, k_2, and η) across diverse conditions summarized as follows:

- variation of the distances between the two waypoints, $d = 0.5\,m$, $2\,m$, and $5\,m$. The choice of the distance range is intended to encompass a wide range of conditions, from situations necessitating precise maneuvers and short-distance waypoints, to those involving coarse-grained and long-distance waypoints.
- variation of $\tilde{\theta}_{init}$, ranging from 5° to 175° at 10° intervals, signifies the various initial heading before moving to the next waypoint.

The evaluation of the triggering conditions of the proposed event-triggered controller is implemented in a discrete manner due to the periodic nature of the state estimation system, which is realized by the localization system that processes sensor data. In the following sections, we present results for a scenario where the triggering condition was evaluated at 5 Hz, which is the control frequency of the current implementation of our system. This frequency was chosen to guarantee the safety of robot operations within its environment. However, depending on the computational capacity of the system, it is possible to evaluate the triggering conditions at higher frequencies.

In simulations, the maximum admissible linear velocity, $u^1_{\max}$, was set to $0.5\,m/s$, reflecting the standard speed at which we operate our mobile robot within a dynamic industrial or enterprise environment, alongside humans and other moving devices. We have also determined a stopping criterion indicating that the neighborhood of the set $\mathcal{O}$ is stabilized, whose threshold is set to $\varepsilon = 0.1\,m$, a reasonable value compared to the size of our mobile robot. In every single run, the robot starts from a specific initial pose (according to the simulation condition such as waypoint distance and initial heading) and heads towards a desired waypoint located at the origin $(0, 0)$.

The selection of k_1, k_2, and η is interdependent, as their values must meet specific criteria to guarantee the stability of the controller, as outlined in (7) and (8). Therefore, we have first determined the range of k_1 values to be evaluated as [1, 15], which covers the potential candidates that guarantee the appropriate performance of the controller. The values of k_2 and η were sequentially chosen within a range of ratios relative to their respective minimum bounds, denoted by $k_{2,min}$ and η_{min} and known by the right-hand side of (7) and (8) respectively. The selected upper bounds for k_2 and η values were set by the maximum ratio defined as: $k_{2,max}/k_{2,min} = 3$ and $\eta_{max}/\eta_{min} = 2$, determined by preliminary simulation results.

For each of the above-mentioned conditions we computed the three evaluation metrics for every set of the selected control parameters. We then assigned a score to each candidate set of parameters by combining the three metrics normalized individually with respect to the best ones among all the candidates, with different weights (w_s, w_d and w_h).

The formula for scoring each candidate set of parameters is

$$\text{Score}^i = w_s \frac{m_s^i}{m_{s,max}} - w_d \frac{m_d^i}{m_{d,min}} - w_h \frac{m_h^i}{m_{h,min}} \quad (11)$$

where m_s^i, m_d^i and m_h^i are three evaluated metrics calculated for the i-th candidate, and $m_{s,max}$, $m_{d,min}$ and $m_{h,min}$ represent the best metrics among all the candidate parameter sets under the same simulation condition. We then consider the following 2 cases for choosing the weights:

Case1: Prioritizing the average speed of reaching the goal, where w_s was selected to have the maximum value compared to the weights of the other two metrics.

Case2: Prioritizing the shorter overall traveled distance, where w_d was chosen to have the maximum value compared to the weights of the other two metrics.

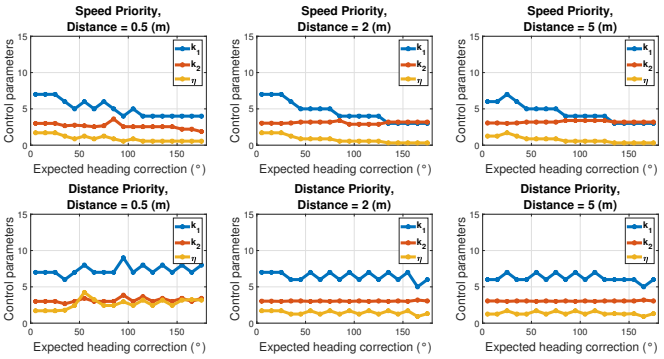

Figure 1: Optimal values of control parameters k_1, k_2 and η for the designed controller. Top-row results are for a controller prioritizing the average speed, whereas bottom row shows the results prioritizing the shorter traveled distance.

The results of the optimal control parameters that yield the best performance based on our introduced metrics are summarized in Figure 1. The results indicate the following:

When prioritizing speed

- There is a reverse correlation between both the best k_1 and η values and the expected heading correction, $\tilde{\theta}_{init}$, meaning that higher k_1 and η values contribute to better performance for smaller $\tilde{\theta}_{init}$, regardless of the waypoint distances.
- For large waypoint distances, k_2 remains relatively constant regardless of $\tilde{\theta}_{init}$ value. However, for the short waypoint distance ($d = 0.5\,m$), it tends to decrease as $\tilde{\theta}_{init}$ increases. With a few exceptions for large heading corrections, the value of k_2 is smaller than k_1.

When prioritizing distance

- We observe fewer variations in k_1 and k_2 values across different waypoint-distance and heading conditions.
- In general, η values are larger compared to when prioritizing speed, indicating a stronger inclination to reduce speed when the robot's heading deviates from the direction toward the goal.

The trend of evaluation metric results for the periodic controller, executed at 5 Hz, is outlined in Table I within rows linked to the Periodic Controller. In this context, the initial expected heading corrections, $\tilde{\theta}_{init}$, range from 5° to 175°, with the optimal gains chosen based on prioritizing the speed or distance indicators. It can be seen that, regardless of priority type, the performance indicators are initially aligned for small $\tilde{\theta}_{init}$. As $\tilde{\theta}_{init}$ increases, both the distance and heading indicators increase, whereas the speed indicator decreases. This is because larger deviations in the robot's heading from the goal result in reduced linear velocity. Also, when the robot's heading significantly deviates from the goal, the heading indicator increases, and consequently leads to a greater traveled distance to correct the deviation.

VI. Event-Triggered Simulation Results

This section presents the simulation results of the designed ET controller. We use the pre-tuned control parameters detailed in Section V that provides the best performance under the same simulation conditions (*i.e.*, d and $\tilde{\theta}_{init}$). The ET supervision function given by (9) is evaluated at 5 Hz, the same frequency as we run the periodic controller. As for the ET parameters, ε determines the stopping neighborhood of the waypoint when the robot approaches it, selected with the same value as for the periodic controller, $\varepsilon = 0.1$. Although the selection of α and γ impacts the performance (*i.e.*, evaluation metrics) of the ET controller, this paper does not delve into analyzing their effects. The range of α evaluated is $(0, 1]$ with 0.1 intervals, while γ ranges from 1 to 20 with predefined steps determined through simulations. As α increases, the supervision condition becomes more strict with control instances being triggered more frequently. As for the impact of γ, by imposing higher γ values, the triggering condition becomes more stringent regarding heading correction toward the goal.

To assess the performance of the ET controller, we select the best ET parameters using a similar approach presented in Section V. We select the best pair of α and γ parameters which maximizes the performance indicator scores as defined in (11), and derive the associated Triggering Frequency (TF). The trend of the evaluation metric results of the ET controller and the associated average TF are shown in Table I within rows linked to the ET controller.

As depicted in the results presented in Table I, the average TF across various scenarios is below 5 Hz, lower than the frequency at which the periodic controller performs. This demonstrates the effectiveness of the proposed ET controller in reducing communication load while maintaining evaluation metrics comparable to those of the periodic controller, referring to ET Controller row of Table I. Another observation is that the number of triggers is lower for longer waypoint distances, but we did not observe any direct influence of $\tilde{\theta}_{init}$ on the TF.

d	$\tilde{\theta}_{init}$	Priority	Controller	Evaluation Metrics			Average TF (Hz)
				m_s	m_d	m_h	
$0.5\,m$	$5^\circ \rightarrow 175^\circ$	Speed	Periodic	0.9884 ↘ 0.4027	1.0003 ↗ 1.1523	0.1040 ↗ 0.9611	-
			ET	0.9969 ↘ 0.3711	1.0003 ↗ 1.1596	0.1049 ↗ 0.9183	3.07
		Distance	Periodic	0.9884 ↘ 0.3324	1.0003 ↗ 1.0159	0.1040 ↗ 0.9273	-
			ET	0.9969 ↘ 0.3099	1.0003 ↗ 1.0002	0.1049 ↗ 0.9209	3.70
$2\,m$	$5^\circ \rightarrow 175^\circ$	Speed	Periodic	0.9979 ↘ 0.7684	1.0001 ↗ 1.0747	0.1009 ↗ 0.9224	-
			ET	0.9993 ↘ 0.7953	1.0001 ↗ 1.0776	0.1009 ↗ 0.9248	3.41
		Distance	Periodic	0.9979 ↘ 0.7236	1.0001 ↗ 1.0144	0.1009 ↗ 0.9254	-
			ET	0.9993 ↘ 0.7219	1.0001 ↗ 1.0130	0.1009 ↗ 0.9242	3.49
$5\,m$	$5^\circ \rightarrow 175^\circ$	Speed	Periodic	0.9990 ↘ 0.8926	1.0000 ↗ 1.0300	0.1003 ↗ 0.9205	-
			ET	0.9998 ↘ 0.9108	1.0000 ↗ 1.0300	0.1003 ↗ 0.9205	2.88
		Distance	Periodic	0.9990 ↘ 0.9245	1.0000 ↗ 1.0055	0.1003 ↗ 0.8701	-
			ET	0.9998 ↘ 0.8702	1.0000 ↗ 1.0055	0.1003 ↗ 0.9224	2.50

Table I: Evaluation metric and average triggering frequency (TF) results of the periodic (5 Hz) and event-triggered controller, with various simulation conditions regarding the waypoint distances (*i.e.*, d) and the expected heading corrections (*i.e.*, $\tilde{\theta}_{init}$). When $\tilde{\theta}_{init}$ is evolved from 5° to 175°, minimum and maximum results for each individual metric are given, with the evolution being increased if indicated by $\nearrow$, or decreased by $\searrow$.

VII. Conclusion

In this work, the stabilization problem of the position of a wheeled mobile robot based on unicycle dynamics was solved. Relaxing the regulation goal, a bounded control was synthesized, which guarantees for the robot a global approaching of the origin in x and y coordinates. To study the stability properties of the closed-loop nonlinear system, a simple strict Lyapunov function was found. To integrate the proposed control law into a networked navigation system (a centralized planner/supervisor), an event-triggering realization of the algorithm was developed. The influence on the regulation performance of the controller tuning was investigated. Simulations illustrate the comparative performance and reduction in communication load achieved by employing ET regulation in the designed controller in contrast to the periodic controller. Future work could explore dynamic and adaptable control parameters at each step during the transition from one waypoint to another. We also plan to investigate robustness properties against external disturbances and delays, as well as integrating sampled state measurements and an observer into the design.

References

[1] I. Kolmanovsky and N. McClamroch, "Developments in nonholonomic control problems," *IEEE Control Systems Magazine*, vol. 15, no. 6, pp. 20–36, 1995.

[2] F. Lamnabhi-Lagarrigue, A. Annaswamy, S. Engell, A. Isaksson, P. Khargonekar, R. M. Murray, H. Nijmeijer, T. Samad, D. Tilbury, and P. Van den Hof, "Systems and Control for the future of humanity, research agenda: Current and future roles, impact and grand challenges," *Annual Reviews in Control*, vol. 43, pp. 1–64, 2017.

[3] R. Brocket, *Differential Geometric Control Theory*, ch. Asymptotic Stability and Feedback Stabilization, pp. 181–208. Boston: Birkhauser, 1983.

[4] C. C. de Wit, H. Khennouf, C. Samson, and O. J. Sordalen, *Recent Trends in Mobile Robots*, ch. Nonlinear control design for mobile robots, pp. 121–156. World Scientific, 1994.

[5] M. Aicardi, G. Casalino, A. Bicchi, and A. Balestrino, "Closed loop steering of unicycle like vehicles via Lyapunov techniques," *IEEE Robotics & Automation Magazine*, vol. 2, no. 1, pp. 27–35, 1995.

[6] A. Astolfi, "Discontinuous control of nonholonomic systems," *Systems & Control Letters*, vol. 27, no. 1, pp. 37–45, 1996.

[7] Z. P. Jiang and H. Nijmeijer, "Tracking Control of Mobile Robots: A Case Study in Backstepping," *Automatica*, vol. 33, no. 7, pp. 1393–1399, 1997.

[8] D. Kostic, S. Adinandra, J. Caarls, N. Van De Wouw, and H. Nijmeijer, "Collision-free tracking control of unicycle mobile robots," in *Proceedings of the 48th IEEE Conference on Decision and Control held jointly with the 2009 28th Chinese Control Conference*, (Shanghai), pp. 5667–5672, 2009.

[9] B. d'Andréa Novel, G. Campion, and G. Bastin, "Control of nonholonomic wheeled mobile robots by state feedback linearization," *The International Journal of Robotics Research*, vol. 14, no. 6, pp. 543–559, 1995.

[10] A. De Luca, G. Oriolo, and C. Samson, *Robot Motion Planning and Control*, ch. Feedback control of a nonholonomic car-like robot, pp. 171–253. Springer, 1998.

[11] W. Dixon, D. M. Dawson, E. Zergeroglu, and A. Behal, *Nonlinear Control of Wheeled Mobile Robots*. Lecture Notes in Control and Information Sciences, London: Springer-Verlag, 2001.

[12] W. J. Evers and H. Nijmeijer, "Practical stabilization of a mobile robot using saturated control," in *Proceedings of the 45th IEEE Conference on Decision and Control*, (San Diego), pp. 2394–2399, 2006.

[13] K. Do, "Bounded controllers for global path tracking control of unicycle-type mobile robots," *Robotics and Autonomous Systems*, vol. 61, no. 8, pp. 775–784, 2013.

[14] E. A. Martínez, H. Ríos, and M. Mera, "Robust tracking control design for unicycle mobile robots with input saturation," *Control Engineering Practice*, vol. 107, p. 104676, 2021.

[15] S. Tatikonda and S. Mitter, "Control under communication constraints," *IEEE Transactions on Automatic Control*, vol. 49, no. 7, pp. 1056–1068, 2004.

[16] P. Tabuada, "Event-Triggered Real-Time Scheduling of Stabilizing Control Tasts," *IEEE Transactions on Automatic Control*, vol. 52, no. 9, pp. 1680–1685, 2007.

[17] M. Lemmon, *Networked Control Systems*, ch. Event-Triggered Feedback in Control, Estimation, and Optimization, pp. 293–358. Springer, 2010.

[18] A. Girard, "Dynamic triggering mechanisms for event-triggered control," *IEEE Transactions on Automatic Control*, vol. 60, no. 7, pp. 1992–1997, 2015.

[19] R. Postoyan, P. Tabuada, D. Nesić, and A. Anta, "A framework for the event-triggered stabilization of nonlinear systems," *IEEE Transactions on Automatic Control*, vol. 60, no. 4, pp. 982–996, 2015.

[20] R. Postoyan, M. C. Bragagnolo, E. Galbrun, J. Daafouz, D. Nesić, and E. B. Castelan, "Event-triggered tracking control of unicycle mobile robots," *Automatica*, vol. 52, pp. 302–308, 2015.

[21] P. Zhang, T. Liu, and Z.-P. Jiang, "Tracking control of unicycle mobile robots with event-triggered and self-triggered feedback," *IEEE Transactions on Automatic Control*, vol. 68, no. 4, pp. 2261–2276, 2023.

[22] K. Khalil, *Nonlinear Systems Third Edition*. Prentice Hall, 2002.